

Coiled coil peptide induced organization of gold nanoparticles mediated by electrostatic interactions

Sara C. Wagner,[#] Meike Roskamp,[§] Helmut Cölfen,[¥] Christoph Böttcher,[§] Sabine Schlecht,^{*,§} and Beate Koksch^{*,#}

[#]*Institute of Chemistry and Biochemistry - Organic Chemistry, Freie Universität Berlin, Takustrasse 3, 14195 Berlin, Germany, [§]Institute of Chemistry and Biochemistry - Inorganic Chemistry, Freie Universität Berlin, Fabeckstrasse 34-36, 14195 Berlin, Germany, [¥] Institute of Chemistry and Biochemistry - Research Center for Electron Microscopy, Freie Universität Berlin, Fabeckstrasse 36a, 14195 Berlin, Germany, and ^{*}Department of Colloid Chemistry, Max-Planck-Institute of Colloids and Interfaces, Research Campus Golm, Am Mühlenberg, 14424 Potsdam, Germany*

Discussion of analytical ultracentrifugation measurements.

The molecular weight determined from integration of the diffusion corrected molar mass distribution from sedimentation velocity experiments matches the value of a trimer (10489 g/mol) for VW05 and a monomer (3496 g/mol) for VW05-ref. The determined M_w 's are 10130 g/mol (300 μ M), 11080 g/mol (100 μ M) and 9790 g/mol (50 μ M) for VW05 and 3380 g/mol (400 μ M), 3540 g/mol (200 μ M) and 3980 g/mol (50 μ M) for VW05-ref (see Figure S4a).

The sedimentation equilibrium results of $M_w = 9960$ g/mol (35,000 rpm) resp. $M_w = 9470$ g/mol (40,000 rpm) from the extrapolation of $1/M_{w,app}$ to $c = 0$ (Figure S4b) also suggest the existence of a trimer for VW05 consistent with the results from sedimentation velocity, although the absolute values are by about 10 % too low. For VW05-ref, $M_w = 3500$ g/mol was obtained for 40,000 and 45,000 and rpm consistent with the monomer.

WINNOLIN v. 1.06 (Yphantis et al. 1997) was independently used to prove the existence of trimers for VW05. The data have been fitted globally to a non interacting ideal species model over the entire investigated concentration range and three

speeds giving a M_w of 11000 g/mol consistent with the trimer (data shown for 300 $\mu\text{M}/\text{ml}$ to give an overview, Figure S4c). The fitted curve for a single species fits well with the data, differences are caused by material loss at higher speed.

For VW05-ref, the fitted curve for a single species fits well with the data and the resulting value for sigma 0.4842 corresponds to a molecular weight of a monomer (3020 g/mol, data shown for 300 $\mu\text{M}/\text{ml}$ to give an overview, Figure S4d).

For both peptides a diagnostic plot for reversible self association was set up by plotting $M_{w,\text{app}}$ as determined for each radial position and thus each concentration present in the ultracentrifuge cell against the local concentrations in the ultracentrifuge cell for each of the loading concentrations. The absence of a master curve shows the absence of reversible self association for VW05 and VW05-ref.

Supporting information-Additional Figures.

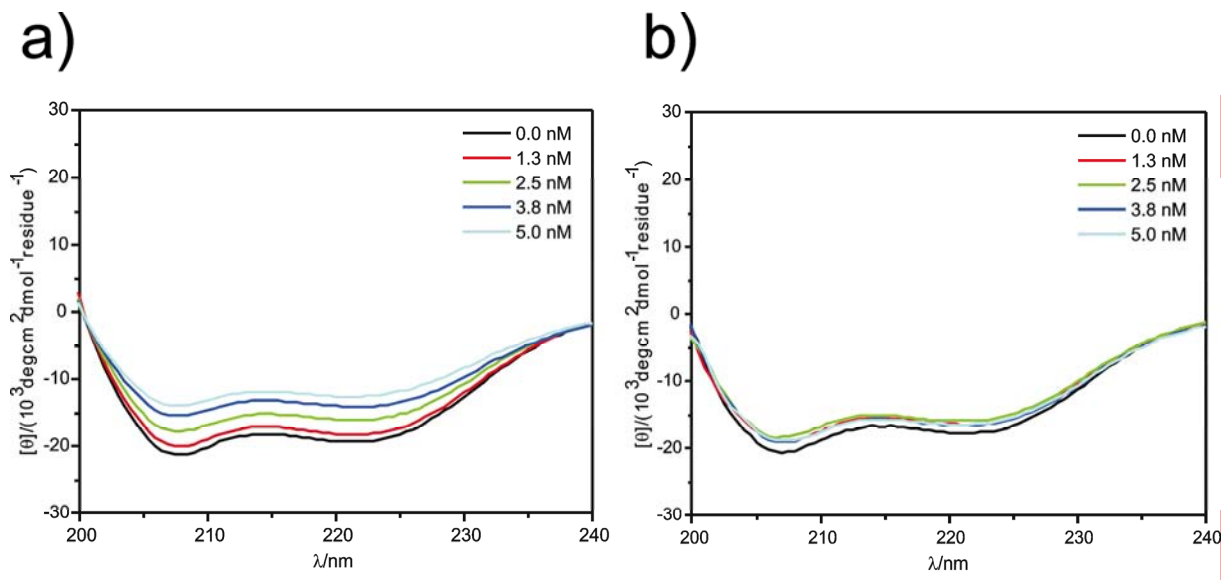


Figure S1. Circular dichroism spectra of 50 μM VW05 (a) in 10 mM Tris/HCl buffer (pH 9.0) and (b) in 10 mM phosphate/NaOH buffer (pH 12.0) at different concentrations of Au/MUA nanoparticles. Scattering effects of the formed aggregates causes a gradual decrease of CD intensity with a higher concentration of nanoparticles at pH 9.0.

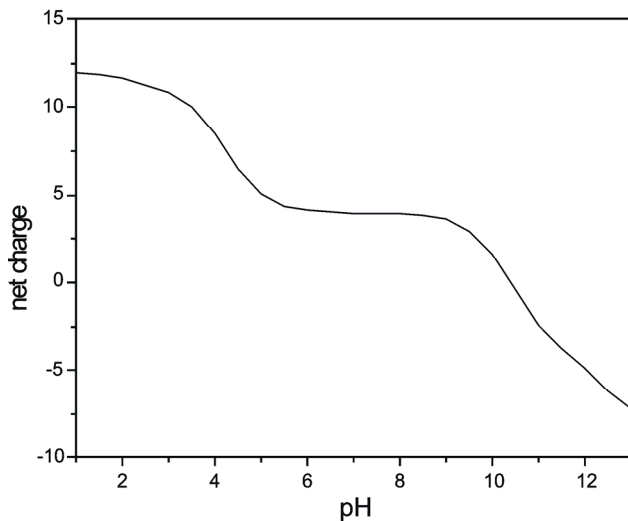


Figure S2. pH Dependence of the peptides net charge which has been calculated using the EMBL WWW Gateway to Isoelectric Point Service (<http://www.embl-heidelberg.de/cgi/pi-wrapper.pl>).

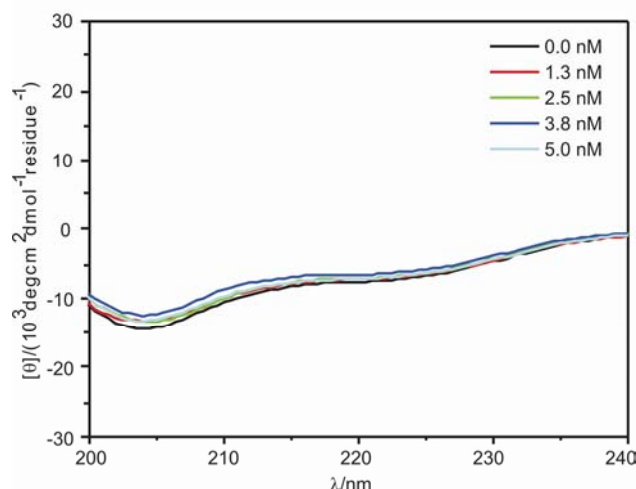


Figure S3. Circular dichroism spectra of 50 μM VW05-ref in 10 mM Tris/HCl buffer (pH 9.0) at different concentrations of Au/MUA nanoparticles.

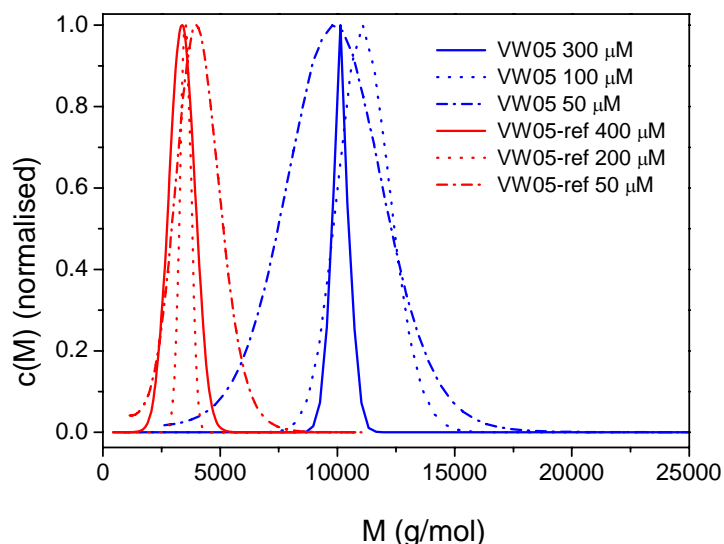


Figure S4a. Molar mass distributions $c(M)$ for different concentrations of VW05 and VW05-ref from sedimentation velocity. Note that due to the small peptide size, the diffusion correction, especially for the small concentrations, was not entirely successful and the distributions are too broad.

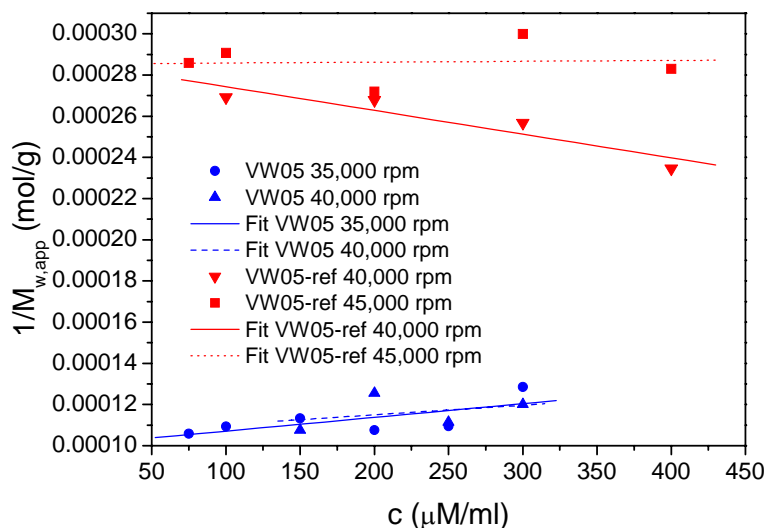


Figure S4b. Plot of the concentration dependence of the inverse apparent weight average molecular weight $M_{w,app}$ vs loading concentration as evaluated with the MSTAR program.

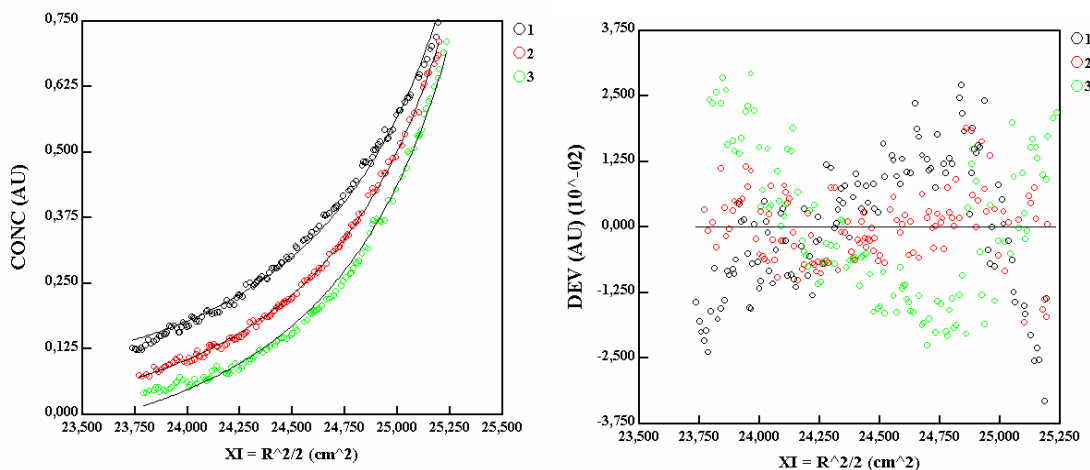


Figure S4c. Left: WINNONLIN fits of the experimental concentration profiles for VW05 at 35,000, 40,000 and 45,000 rpm. Right: residuals of the fits.

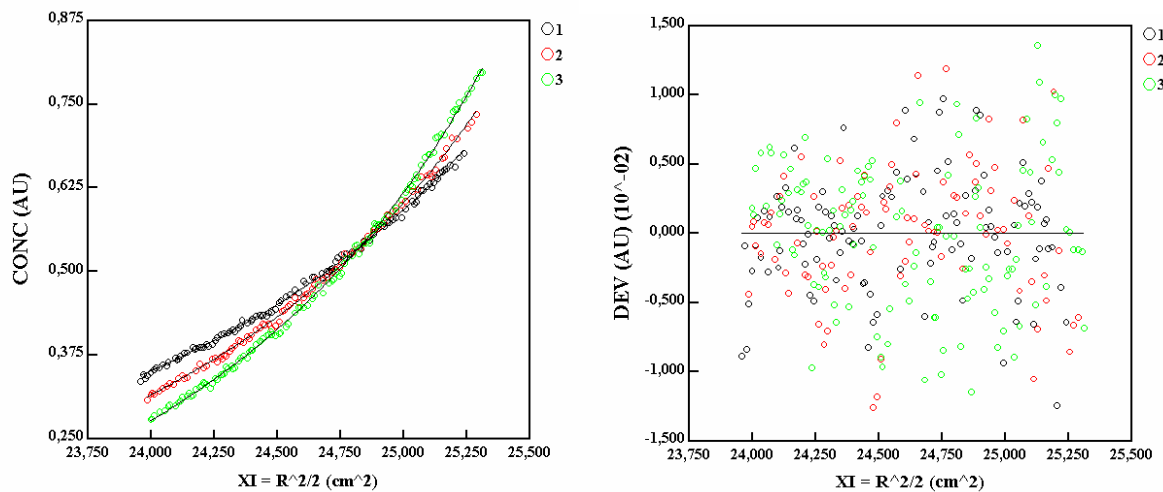


Figure S4d. Left: WINNONLIN fits of the experimental concentration profiles for VW05-ref at 40,000, 45,000 and 50,000 rpm. Right: residuals of the fits.

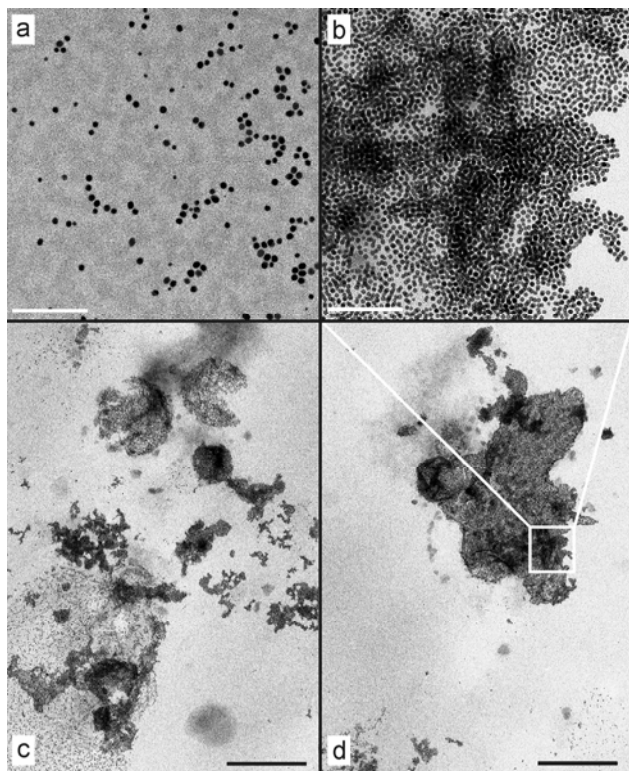


Figure S5. TEM micrographs of (a) isolated Au/MUA nanoparticles at pH 9.0 and (c and d) large assemblies of Au/MUA nanoparticles in presence of VW05. (b) Magnified detail from (d) indicating multilayered organization of the VW05-mediated aggregates (white scale bars: 50 nm, black scale bars: 500 nm). The superposition of manifold particle layers is a prominent feature of the aggregates and differs significantly from the monolayers that are obtained from pure nanoparticle preparations (Figure S5b). These features point to the formation of peptide-mediated nanoparticle networks in aqueous solution. Multiple particle layers likely reflect the collapse of peptide-nanoparticle aggregates upon sample drying. The assemblies coexist with a minor fraction of loosely dispersed nanoparticles which are obviously not involved in the peptide-mediated aggregation.

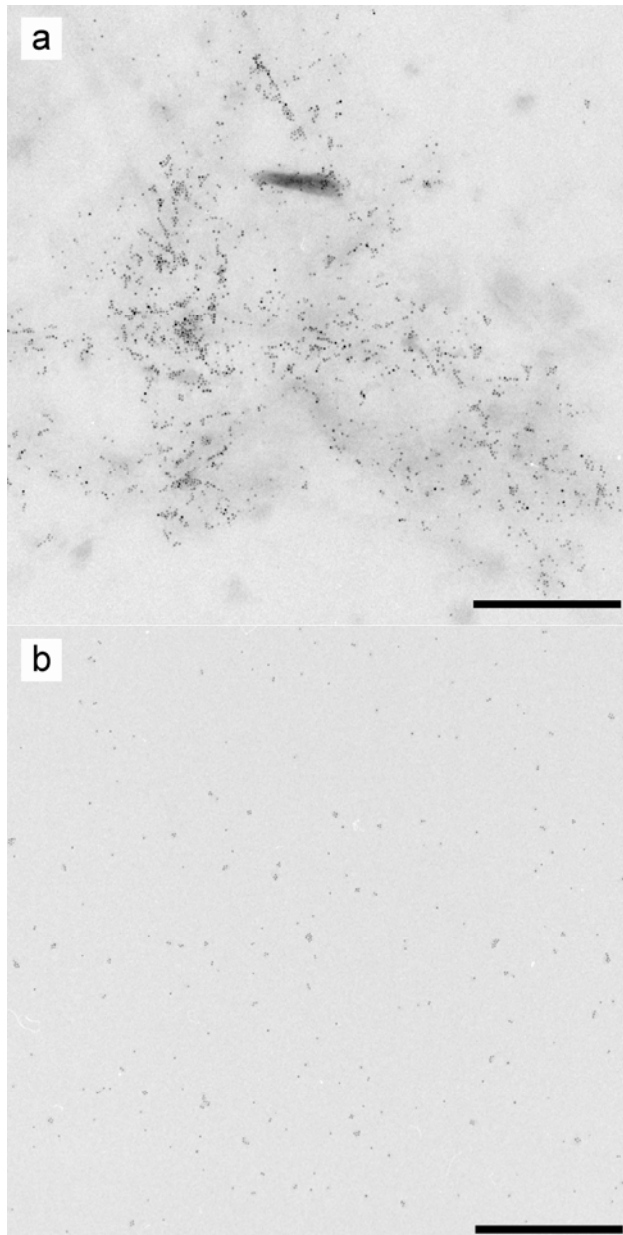


Figure S6. TEM micrographs of Au/MUA nanoparticles (a) in absence and (b) in presence of VW05 at pH 12 (scale bars: 500 nm).

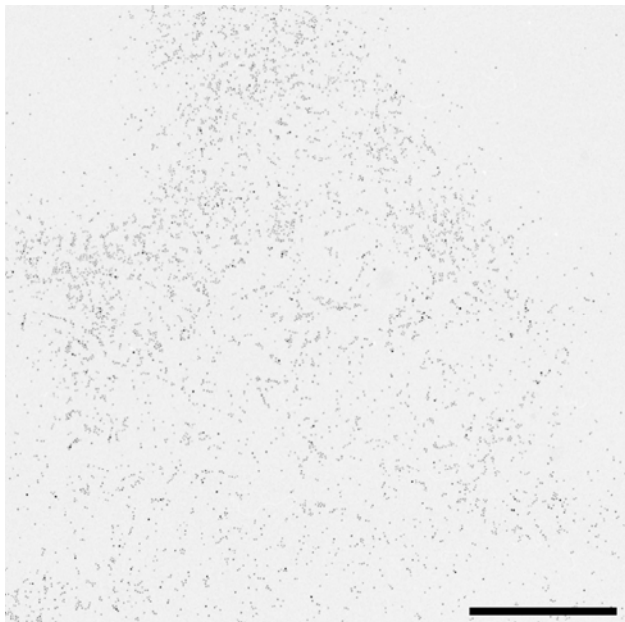


Figure S7. TEM micrographs of Au/MUA nanoparticles in presence of VW05-ref at pH 9 (scale bar: 500 nm).

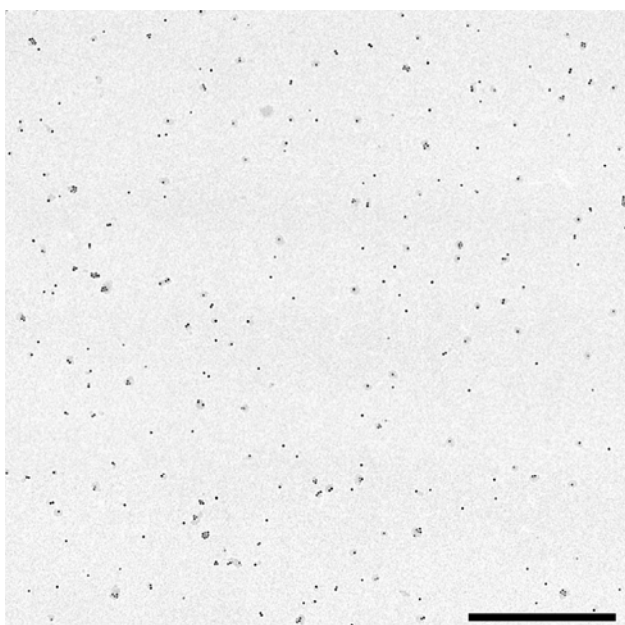


Figure S8. TEM micrographs of Au/MUA nanoparticles in presence of VW05 after changing the pH value of 9 to 12 (scale bar: 500 nm). The sample was allowed to incubate for 10 minutes after pH change. The efficient aggregation of nanoparticles before changing the pH value was controlled by TEM measurements (data here not shown).